CHEMISTRY
A EUROPEAN JOURNAL

DOI: 10.1002/chem.201001683

# [Ln(binolam)$_3$]·(OTf)$_3$, a New Class of Propeller-Shaped Lanthanide(III) Salt Complexes as Enantioselective Catalysts: Structure, Dynamics and Mechanistic Insight**

**Lorenzo Di Bari,*[a] Sebastiano Di Pietro,[a] Gennaro Pescitelli,[a] Fernando Tur,[b] Javier Mansilla,[b] and José M. Saá*[b]**

**Abstract:** The ligand 3,3′-bis(diethylaminomethyl)-1,1′-bi-2-naphthol (binolam) contains an arrayed Brønsted acid–Brønsted base (BABB) system, which is responsible for the original shape of its lanthanide compounds. The solution structure of Pr, Nd and Yb compounds is solved by means of paramagnetic NMR spectroscopy and it is demonstrated that they are substantially isostructural, but with a completely new fold compared to the apparently similar heterobimetallic systems based on 1,1′-bis(2-naphthol) (binol) and alkali cations. The aromatic nuclei lie in a region equatorial with respect to the $C_3$ symmetry axis, whereas the alkylamine chain stretches almost parallel to $C_3$, above (and below) $Ln^{3+}$. This is also found in the crystal structure of the binolamo–scandium complex. A detailed study of the proton-exchange processes within the network of BABBs present in the complex is reported, which provides insight into the mechanism of the enantioselective Henry reaction promoted by these systems.

**Keywords:** binol derivatives · circular dichroism · enantioselectivity · lanthanides · NMR spectroscopy

## Introduction

A new family of lanthanide(III) salt complexes derived from 3,3′-bis(diethylaminomethyl)-1,1′-bi-2-naphthol (binolam, **1**; see Scheme 1) has been recently proposed as a multifunctional system for enantioselective catalysis.[1,2] At first glance they recall the heterobimetallic complexes introduced by Shibasaki,[3] which found numerous applications as

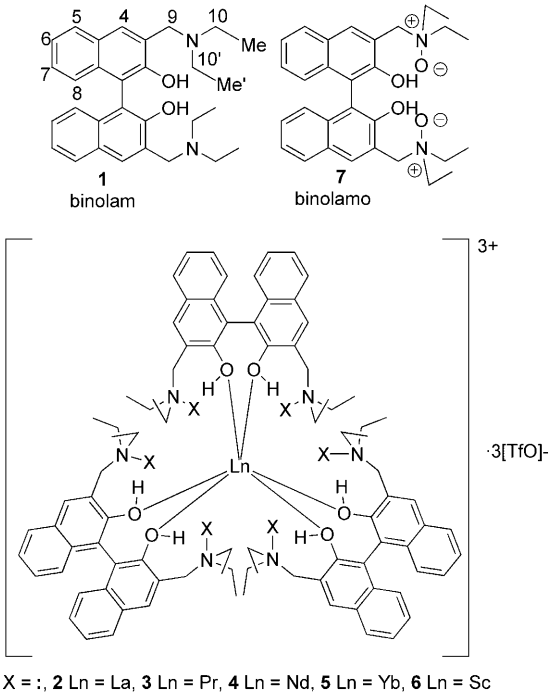


Scheme 1. Structural formulae of binolam **1**, binolamo **7** and their 3:1 complexes with Ln(OTf)$_3$.

[a] Prof. L. Di Bari, S. Di Pietro, Dr. G. Pescitelli
Dipartimento di Chimica e Chimica Industriale
via Risorgimento 35, 56126 Pisa (Italy)
Fax: (+39) 0-502-219-260
E-mail: ldb@dcci.unipi.it

[b] Dr. F. Tur, J. Mansilla, Prof. J. M. Saá
Departament de Química, Universitat de les Illes Balears
Ctra. Valldemossa, Km. 7,5, 07122 Palma de Mallorca (Spain)
Fax: (+34) 9-711-734-26
E-mail: jmsaa@uib.es

[**] Ln = La, Pr, Nd, Yb; binolam = 3,3′-bis(diethylaminomethyl)-1,1′-bi-2-naphthol; OTf = triflate.

Supporting information for this article is available on the WWW under http://dx.doi.org/10.1002/chem.201001683. It contains NMR spectra ($^1$H, HSQC, EXSY, DOSY) of binolam and its $Ln^{3+}$ compounds; experimental and calculated paramagnetic shifts; conformational data; thermogravimetric analysis; and ESI-MS spectra.

enantioselective catalysts,[4] and prompted a set of structural and dynamic investigations owing to their intriguing properties.[5–8]

One of the keys to the success of heterobimetallic systems has been attributed to the coexistence in the same molecule of Lewis acid and Brønsted base centres. The latter arise because the organic ligand becomes deprotonated by a base before or during synthesis of the complex. Consequently, the system is described as $[M_3Ln(binolate)_3]$ (binolate = 1,1′-bis(2-naphthoate)) with explicit reference to the alkali metal ion M, which constitutes O-M-O bridges between nearby binolate units, not only in the solid state but also in solution. This has been demonstrated by means of paramagnetic NMR spectroscopy and near-IR (NIR) circular dichroism (CD), at least for the Yb complex: both magnetic and optical spectra are strongly dependent on the alkali metal.[5,7]

From this point of view, binolam **1** appears to be a promising alternative to 1,1′-bis(2-naphthol) (binol) for the complexation of lanthanide triflate salts $Ln(OTf)_3$,[9] because it incorporates basic tertiary alkyl amine groups. In fact, reaction of binolam **1** with $Ln(OTf)_3$ (Ln = La, Pr, Nd, Yb), as well as with $Sc(OTf)_3$, does not require the use of external bases and proceeds with excellent yields to one family of products **2**–**6** with formula $[Ln(binolam)_3]\cdot(OTf)_3$ (Scheme 1), and no trace of different stoichiometries is apparent from the $^1$H NMR spectra.[10] In contrast to the anionic lanthanide complexes of Shibasaki (with cationic counterions), Saá's lanthanide complexes can be defined as cationic (with anionic counterions) since no proton loss is detected, as demonstrated through fast atom bombardment mass spectrometry, ESI-MS and $^1$H NMR integrals.[2] This has two relevant consequences. In the first place, Saá's complexes do not incorporate alkali metal ions, which played a central role in determining the structure of Shibasaki's $M_3Ln(binolate)_3$ holding together the organic ligands.[5,7] Secondly, Saá's complexes $[Ln(binolam)_3]\cdot(OTf)_3$ can be depicted as sharing a Lewis acid (the lanthanide), a Brønsted acid (the hydroxy group) and a Brønsted base (the amine), or a LABABB network. To what extent the hydroxyl proton is really engaged in hydrogen bonding with the nearby amine nitrogen atom is a question that will be discussed later on.

When the racemic ligand is used, one should envisage the formation of diastereomeric species of the type *R*,*R*,*R* versus *R*,*R*,*S*, that is, homo- versus heterochiral. The symmetry classes of the two species are radically different: at the highest, *R*,*R*,*S* can be $C_2$ and three sets of, for example, aromatic resonances should be distinguished by NMR spectroscopy, whereas *R*,*R*,*R* can be $D_3$ leading to only one set of signals.[5,6] It is easy to demonstrate that only the latter is the case for $[Ln(binolam)_3]\cdot(OTf)_3$ complexes, and that there is no evidence of heterochiral species formation. This is true for all the lanthanides investigated (which go across the whole transition series), together with the closely related scandium, and is in strong contrast to the heterobimetallic complexes, in which there is variable proportion of homo- and heterochiral species, according to Ln and M.[5]

As we shall see in the following discussion, there are very profound chemical and structural differences between $[Ln(binolam)_3]\cdot(OTf)_3$ and $M_3Ln(binolate)_3$ complexes and the former must be considered a completely new class of compounds, for which some applications as enantioselective catalysts have already been uncovered. Their possible role as enantioselective catalysts will probably need further investigation, which we hope the present work will stimulate. The N-oxide derivative of ligand **1**, binolamo **7**, has also been shown to be capable of forming the interesting series of complexes $[Ln(binolamo)_3]\cdot(OTf)_3$, closely related to those derived from binolam, for which no applications in asymmetric catalysis have yet been reported. Herein, we report only the scandium complex **8**, useful for our purposes in the structural investigation.[11]

## Results and Discussion

**Structure of ligand 1**: Binolam (**1**) is an aminophenol, for which an intramolecular hydrogen bond leads to a six-membered cycle.[9] Depending on the relative strength of the O–H and $N^+$–H bonds, the hydrogen atom may be located nearer to the hydroxy or amino group. In water, the $pK_A$ values of 2-naphthol and benzyldimethylammonium can be estimated as about 9.3 and 8.9, respectively; however, the difference is likely to be much larger in acetonitrile with the ammonium ion being the stronger acid by several orders of magnitude of $K_A$.[12,13] This indicates that the cycle should be best depicted as in Scheme 2 for compound **9**, which represents the individual naphtholamine moieties in binolam **1**.

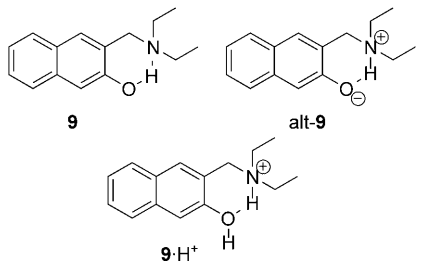


Scheme 2. The two limiting structures for naphtholamine and the result of their protonation.

Such an expectation is confirmed by its X-ray diffraction structure (Figure 1).[14] Two key features of the X-ray structure of binolam **1** are relevant to the present study: 1) the diethylaminomethyl arms appear to be in a rigidified conformation due to the presence of O–H···N bonds (O–H = 1.76 and 1.92 Å ; O···N = 2.67 and 2.63 Å), and 2) the dihedral $C_2$-$C_1$-$C_{1'}$-$C_{2'}$ angle = 90.01°. In addition, DFT geometry optimisations run on **9** at the B3LYP/6-31+G(d+,p) level (see Experimental Section), which is appropriate for describing hydrogen-bonded systems, also converged to such a type of structure.[15] In fact, the O–H···N hydrogen-bonded structure **9** was found to be much more stable (6.8 kcal mol$^{-1}$) with re-

  

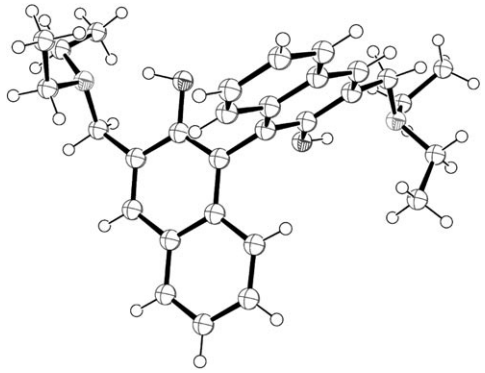

Figure 1. Single-crystal X-ray diffraction structure of binolam **1**.

spect to the absence of H-bonds (i.e., with O–H directed toward C1); moreover, starting from an input structure like *alt*-**9** (with H located on N) led to the same optimised structure as **9**. The protonated species **9**·$H^+$ was instead stabilised by an $N^+$–H···O bond.

We can bring two sets of experimental proofs to show that the same also occurs for binolam **1** in solution, by studying the NMR and UV/Vis CD spectra. The $^1$H NMR spectrum (Figure 2) displays two doublets for the diastereotopic H9 (refer to Scheme 1 for numbering), at 4.18 and 3.95 ppm, two multiplets for H10 at 2.73 and 2.64 ppm, but only one resonance for the methyl groups. Moreover, HSQC features only one resonance for the C10. These facts demonstrate that there is fast nitrogen inversion, which shuffles the two diastereotopic ethyl groups, thus making them isochronous. The large chemical shift difference between the H9 protons reveals hindered rotation and selective exposure to the shielding/deshielding field due to the aromatic ring. The 4.18 ppm resonance results from a proton (H9a) practically coplanar with the ring and eclipsing C4, which is also found in DFT geometries for **9** (C4/C3/C9/H9a dihedral angle ≈13°) and is apparent in the XRD structure shown in Figure 1.

After adding two equivalents of acid (HCl, Figure 2), the NMR spectrum is deeply altered, on account of the positive charge developed on the N atom. The downfield shift of H4, which jumps left of H5, and of all the ethyl chains protons, is remarkable.

The UV/Vis CD spectra of (*S*)-binolam **1** in acetonitrile resemble poorly those of (*S*)-binol in terms of position and relative intensity of bands (Figure 3). However, upon protonation of binolam with excess HCl, its CD spectrum becomes similar to that of binol. In particular, the region between 220 and 250 nm is dominated by exciton coupling[16] between $^1B_b$ transitions[17,18] ($2^1B_{3u}$ in naphthalene)[19] of the 2-naphthol chromophore, which is polarised approximately along the C2–C6 direction.[3,20,21] The resulting CD couplet is very symmetrical for binol and protonated binolam, whereas it is severely altered by superposition with higher-energy $^1B_a$ bands ($2^1B_{2u}$ in naphthalene)[20] for binolam. Less evident differences between binol and binolam are observed in the low-energy region corresponding to $^1L_a$ (280–300 nm) and $^1L_b$ (320–350 nm) transitions (respectively $1^1B_{2u}$ and $1^1B_{3u}$ in naphthalene).[20]

We can conclude that in the neutral ligand **1**, the hydroxyl group is a hydrogen-bond donor, thus increasing the amount of negative charge on the oxygen, whereas the nitrogen is the acceptor. This feature is relevant to the capacity of binolam **1** required to complex lanthanide(III) triflate salts.

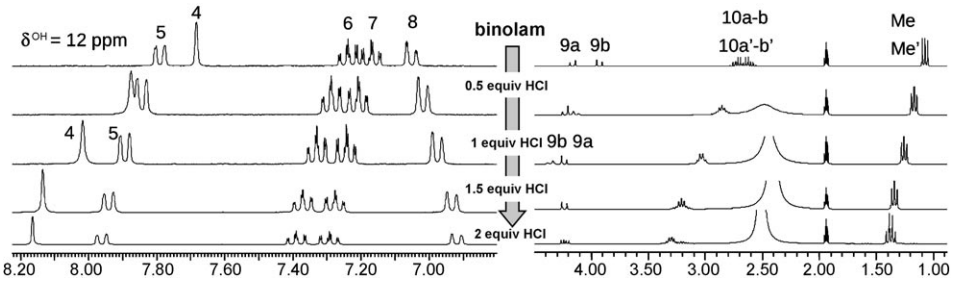


Figure 2. $^1$H NMR spectra of the binolam ligand **1** in $CD_3CN$ after the addition of increasing quantities of HCl.

**Structure of Saá's complexes: static features**: A number of $[Ln(binolam)_3]\cdot(OTf)_3$ complexes **2**–**5** (Ln = La, Pr, Nd, Yb) have been obtained simply by mixing pure binolam (either racemic or enantiopure, 3 equiv) with the appropriate lanthanide triflate salt (freshly dried in vacuo at 220 °C for 96 h; 1 equiv) in dry (freshly

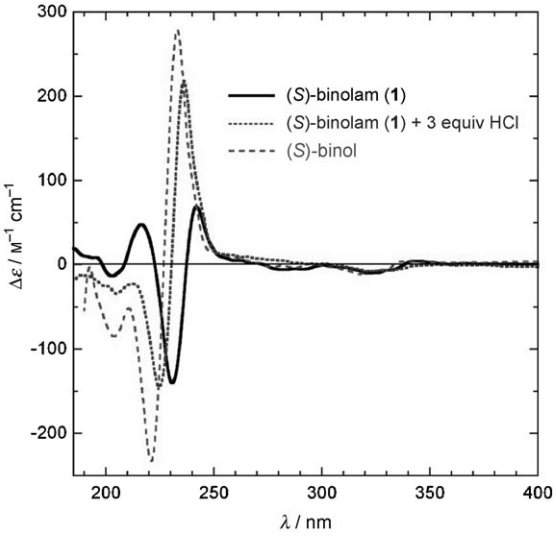


Figure 3. CD spectra of (*S*)-binol, (*S*)-binolam and protonated (*S*)-binolam in acetonitrile.

distilled from $CaH_2$) acetonitrile at room temperature. Removal of the solvent under reduced pressure yielded complexes **2**–**5** as long-term, shelf-stable, orange-brown solids. However, thermogravimetric analysis (25–200 °C, Figure S12 in the Supporting Information) showed that these samples may retain up to 4.6% of residual water (only trace amounts of acetonitrile were detected), as proven by IR and NMR analyses carried out on the initial and final samples. B3LYP calculations using the 6-31G(d) basis set for all non-metallic atoms, and the Stuttgart/Dresden SDD effective-core-potential basis set for lanthanum,[22] support the notion that hydration of $[Ln(binolam)_3]\cdot(OTf)_3$ with two water molecules (which occupy second-sphere coordination sites) is thermodynamically driven by 6.9 kcal mol$^{-1}$. As discussed later on, this residual water present in complexes **2**–**6** is of interest for mechanistic studies. The spectra of the $[La(binolam)_3]\cdot(OTf)_3$ complexes **2**–**5** with Ln = La, Pr, Nd, Yb were obtained in commercial $CD_3CN$, which contains some water and, therefore, they often show some minor contamination by binolammonium salt (resulting from hydrolysis). Lanthanides can achieve coordination numbers larger than six, so it is expected that one or two water molecules can enter the second coordination sphere of the larger lanthanides, thereby inducing hydrolysis when ligands are somewhat basic or an external base is added. Specifically, careful addition of increasing amounts of water to complexes **2**–**6** dissolved in $CD_3CN$ led to hydrolysis (slow for the smaller lanthanides), thereby yielding binolammonium salt and the appropriate lanthanide hydroxide, which appears as a mucus-like flocculating species in the NMR tube. This hydrolytic process is extremely fast when an amine base is present in—or added to—the solution.[23] Apart from this, in each case only one set of resonances is apparent, which demonstrates that we are dealing with fully symmetric species in which all the corresponding atoms and groups are equivalent, that is, the (possibly dynamic) point group must be $D_3$.

A broad resonance at low field integrating for six protons can be recognised in all $^1$H NMR spectra and assigned to the hydroxyl proton. The spectra provide rather sharp lines: only in the case of Nd is there a moderate broadening. This ensures that common correlation techniques (COSY, TOCSY, NOESY) can be used to assign the spectra. A few ambiguities remain concerning the diastereotopic protons and groups, namely those at positions 9, 10 and the methyl groups (notice that the ethyl groups attached to the same nitrogen atom are diastereotopic). Heteronuclear correlation (see the Supporting Information) allowed us to assign the $^{13}$C NMR spectra; the results are shown in Table 1.

Table 1. Assignment of $^1$H and $^{13}$C NMR spectra (ppm) of binolam **1** and $[Ln(binolam)_3]\cdot(OTf)_3$ complexes **2**–**5** in $CD_3CN$ at 25 °C.

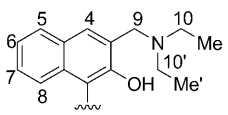


| | Binolam (**1**) | | La (**2**) | | Pr (**3**) | | Nd (**4**) | | Yb (**5**) | |
|---|---|---|---|---|---|---|---|---|---|---|
| Proton | $^1$H | $^{13}$C | $^1$H | $^{13}$C | $^1$H | $^{13}$C | $^1$H | $^{13}$C | $^1$H | $^{13}$C |
| 4 | 7.70 | 128.5 | 7.75 | 131.6 | 6.99 | 128.8 | 8.80 | 131.9 | 3.23 | 122.5 |
| 5 | 7.81 | 128.7 | 7.99 | 129.2 | 7.50 | 127.6 | 8.45 | 128.8 | 5.48 | 124.4 |
| 6 | 7.26 | 123.4 | 7.30 | 123.0 | 6.97 | 123.4 | 7.47 | 127.3 | 5.38 | 121.7 |
| 7 | 7.19 | 126.7 | 7.10 | 127.3 | 6.91 | 126.5 | 7.55 | 124.7 | 5.53 | 123.8 |
| 8 | 7.08 | 124.8 | 6.67 | 125.8 | 6.00 | 126.1 | 7.71 | 127.8 | 1.79 | 121.7 |
| 9a | 4.18 | 58.2 | 2.97 | 56.6 | 1.85 | 55.2 | 1.20 | – | −1.19 | 50.6 |
| 9b | 3.96 | | 2.46 | | 0.40 | | 2.95 | | −4.26 | |
| 10a | 2.74 | 47.4 | 2.94 | 48.4 | 4.78 | 50.0 | 0.59 | 47.5 | 11.32 | 55.1 |
| 10b | | | 2.91 | | 4.45 | | 1.13 | | 10.73 | |
| 10a′ | 2.64 | | 2.86 | 46.5 | 3.19 | 47.2 | 2.17 | 46.0 | 6.19 | 50.4 |
| 10b′ | | | 2.75 | | 3.33 | | 2.49 | | 5.36 | |
| Me | 1.10 | 11.5 | 0.26 | 6.4 | 0.98 | 7.7 | −0.26 | 6.2 | 3.14 | 10.6 |
| Me′ | | | 0.86 | 10.3 | 1.40 | 10.8 | 0.13 | 10.0 | 4.99 | 14.0 |
| OH | 2.16 | | 9.23 | | 11.5 | | – | | 29.0 | |

The large hyperfine shift in the paramagnetic species ensures to a very good extent that formation of heterochiral species (of the type *R*,*R*,*S*) can be ruled out: even in the case of reasonably prompt exchange between diastereomers like *R*,*R*,*R* and *R*,*R*,*S*, the difference in resonance frequencies between corresponding nuclei in the two complexes would be large enough to lead to signal decoalescence and to make the exchange appear slow on the paramagnetic NMR timescale.[6] This point will be further discussed below.

The choice of acetonitrile as the solvent limits somehow the possibility of low-temperature investigations; however, no meaningful broadening of the lines is observed down to −40 °C, which indicates that the $D_3$ symmetry must be regarded as static rather than dynamic.[7]

The situation so far is very similar to that found for the case of heterobimetallic systems $[M_3Ln(binolate)_3]$,[5,7] which may appear not at all surprising on account of the close structural analogy between the two organic ligands, binolate and binolam. On taking a closer look, however, we must observe that there are differences between the spectral data, which demonstrates that the actual solution structures must be profoundly different.

In the first place, let us look at the simple complexation shifts of the aromatic protons in the diamagnetic La complex **2**, and compare them with the data reported in the literature for the corresponding $[M_3La(binolate)_3]$, as shown in Figure 4. Owing to complex formation and to the consequent congestion of three biaryl groups around one centre, the organic ligand nuclei experience a shift, which is largely due to exposure to shielding/deshielding effects of the nearby aromatic rings. It is immediately apparent that the

  

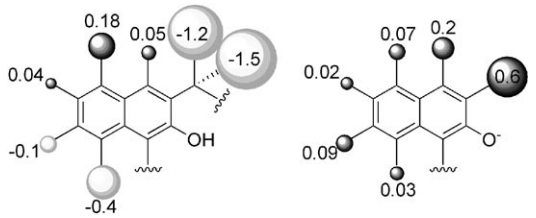


Figure 4. $^1$H NMR complexation shifts of [La(binolam)$_3$]·(OTf)$_3$ (left) versus [Na$_3$La(binolate)$_3$] (right). The dark grey and light grey spheres represent down- and upfield shifts, respectively, with reference to the free ligands (binolam and binolate, respectively). The radii of the spheres are proportional to the displacement between free and bound forms. Owing to the uncertain assignment of the diastereotopic ethyl group resonances, their complexation shifts are not represented.

situation is completely different in the two complexes. The protons in heterobimetallic complex [Na$_3$La(binolate)$_3$] are generally downfield shifted. On the contrary, the protons in [La(binolam)$_3$]·(OTf)$_3$ are divided into two families according to the sign of the effect. In particular, we may notice the very high negative shift of the two H9 protons, [La(binolam)$_3$]·(OTf)$_3$ moving upfield by 1.2 (9a) and 1.5 ppm (9b), which demonstrates their close contact to the centre of a nearby aromatic ring.

**Paramagnetic NMR spectroscopy**: Similarly to what has been done successfully in many other cases, and very notably for [M$_3$Ln(binolate)$_3$], we can obtain an accurate solution structure by analysing the pseudo-contact shifts of paramagnetic lanthanide complexes.[24]

Very briefly, we remind here that the observed shift for an NMR-active nucleus, $i$, in a paramagnetic lanthanide complex can be considered the sum of three contributions: a diamagnetic term, $\delta^{dia}$, which can be very well approximated by the La or Lu analogue, and pseudo-contact and contact terms, $\delta^{pc}$ and $\delta^{con}$, typical of the paramagnetic lanthanide (Ln $\neq$ Gd). The contact term contains little structural information, but it decreases very rapidly with the number of bonds between Ln and $i$,[25] which ensures that in the present case only the 4-position (both C and H) can be strongly affected by this contribution,[26] whereas for the other positions $\delta^{con} \approx 0$ [Eq. (1)]:

$$\delta^{obs} = \delta^{dia} + \delta^{con} + \delta^{pc} \approx \delta^{La} + \delta^{pc} \quad (1)$$

In the case of axial complexes possessing a $C_n$ axis with $n \geq 3$, Equation (2) holds:

$$\delta_i^{pc} = \mathscr{D}_{Ln}\left(\frac{3\cos^2\theta_i - 1}{r_i^3}\right) \quad (2)$$

where $\mathscr{D}_{Ln}$ is the magnetic susceptibility anisotropy of the lanthanide Ln, $r_i$ is the distance between $i$ and Ln, and $\theta_i$ is the polar angle of the vector $\boldsymbol{r_i}$ with respect to the $C_n$ axis; the quantity in parentheses is sometimes called geometrical factor, $GF_i$, which is characteristic of $i$ but independent of the lanthanide. The use of La as the diamagnetic reference is perfectly adequate for the early lanthanides like Pr and Nd, but Lu would be a better choice for Yb. In the present case, we shall see that this has no relevant consequence.

Among the three paramagnetic complexes investigated, we chose to start our analysis from Yb for three reasons. First, for Yb the ratio $\delta^{pc}/\delta^{con}$ is particularly favourable, making the approximation of Equation (1) more stringent also for the 4-position.[25] Second, $\mathscr{D}_{Yb}$ is the largest between Pr, Nd and Yb, which ensures that the $\delta^{pc}$ values are also large and consequently more accurately extracted. Third, the Na and K heterobimetallic Yb binolates are the best characterised ones from the point of view of paramagnetic NMR.[7]

If we compare the $\delta^{pc}$ values of the aromatic protons and carbon atoms for **5** and for [Na$_3$Yb(binolate)$_3$],[27] we notice immediately that they follow a completely different pattern. If the geometric factors of the two species were equal or similar, the two sets of $\delta^{pc}$ values should be proportional, that is, fitted by a straight line passing through the origin, which is clearly not the case.

Once more, this testifies that we are dealing with a different structure. In particular, we can observe that in the present case most pseudo-contact shifts for the aromatic nuclei are *negative*, which means that the naphthalene rings occupy an equatorial region with respect to the symmetry axis. This means that although in [Na$_3$Yb(binolate)$_3$] the chirality axes of the ligands are almost parallel to the $D_3$ axis (vertical), in [Yb(binolam)$_3$]·(OTf)$_3$ **5** they lie on a plane roughly orthogonal to $D_3$.

Such a feature is indeed found in the crystal structure of the closely related system [Sc(binolamo)$_3$]·(OTf)$_3$ **8** (Scheme 1),[28] as illustrated in Figure 5. We have taken it as the starting point for a geometry optimisation through the routine PERSEUS,[7,29] which optimises structural parameters (torsion angles and paramagnetic centre location), as well as the magnetic susceptibility tensor, by minimising the difference between experimental and calculated paramagnetic NMR data (pseudo-contact shifts and relaxation rates).

From the comparison between experimental and calculated values of NMR data in **5** and for a structure calculated from the XRD of **8** without altering the atom coordinates, we can notice that the aromatic resonances are well fitted without altering the XRD coordinates. On the contrary, the alkyl chain shifts are more poorly calculated: they must take a different orientation in solution from that in the solid state. Accordingly, we let the relevant torsion angles free to vary in the structural optimisation through PERSEUS, and obtained a much better fit as shown in Figures 6 and 7. This structure was also validated independently by the analysis of the paramagnetic relaxation rates $\rho^{para}$ (for the resonances table and the $\rho^{para}$ plot, see the Supporting Information). The two ethyl chains are very differently oriented: one is roughly parallel to $D_3$, the other lies skew to it. Such a feature is clearly also reflected in the spectrum of diamagnetic

  

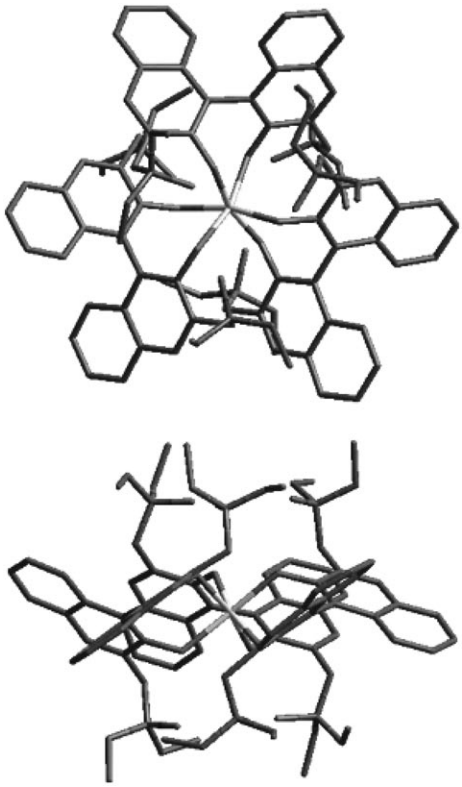

Figure 5. Single-crystal X-ray diffraction structure of $[Sc(binolamo)_3]\cdot(OTf)_3$ (**8**) in which, for the sake of clarity, triflate counterions, solvents ($CH_3CN$ and $H_2O$) and hydrogen atoms have been removed.

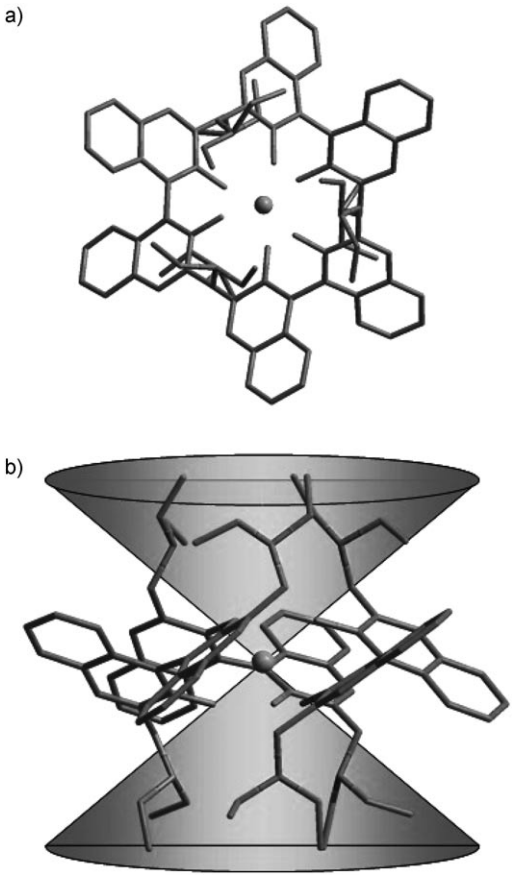


Figure 6. Top (a) and side (b) views of the solution structure of $[Yb(binolam)_3]\cdot(OTf)_3$, obtained through the quantitative analysis of the pseudo-contact shifts as described in the text. In the side view, the shaded cone represents the surface at which the pseudo-contact shifts change sign: nuclei inside the cone are shifted upfield, those lying outside are shifted downfield.

$[La(binolam)_3]\cdot(OTf)_3$, in which the signals of all the nuclei belonging to these two diastereotopic groups are made very strongly anisochronous by a larger or smaller exposure to the ring currents.

The coordination polyhedron is a twisted trigonal antiprism (i.e. a compressed and distorted octahedron). The chirality axis of the bidentate ligand leads to one antipode of the octahedron (remember that the complex incorporates only ligands of the *same* chirality): (*S*)-binolam gives rise to Δ coordination and (*R*)-binolam gives Λ coordination.

Now we can extend this analysis to the lighter paramagnetic elements studied, namely Pr and Nd (**3** and **4**, respectively). Once more, we extracted the paramagnetic shifts of their binolam complexes by subtracting the corresponding values for **2**.

The proportionality between the paramagnetic shifts for different lanthanides (both $^1H$ and $^{13}C$) demonstrates that:

1) the contact contribution can actually be neglected and the paramagnetic shift is indeed a good approximation to $\delta^{pc}$;
2) one and the same set of geometrical factors ($GF_i$) fits the pseudo-contact shifts for the various paramagnetic lanthanides.

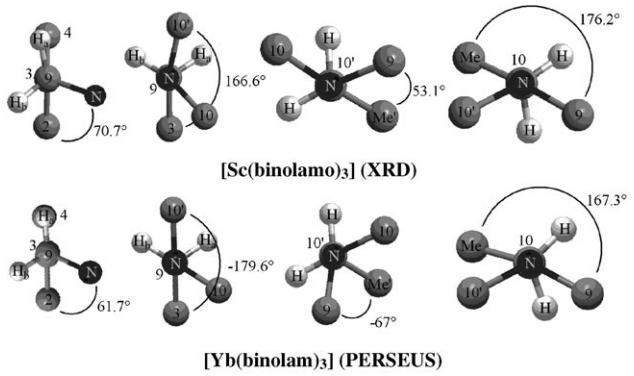


Figure 7. Details of the XRD (top) and PERSEUS-optimised (bottom) structures.

In other words, in a first approximation we can say that the complexes **3**–**5** are isostructural.

The paramagnetic shifts that can be extracted from the data of Table 1 show something that is at odds with expectations: the $\delta^{pc}$ values of Pr and Yb have the same sign, which

  

is in clear contrast to Bleaney's theory,[30] possibly adjusted according to Mironov.[31] In more detail, we should expect that [Eq. (3)]:

$$\mathscr{D}_{Pr}^{theory} : \mathscr{D}_{Nd}^{theory} : \mathscr{D}_{Yb}^{theory} = -0.52 : -0.20 : 1 \quad (3)$$

while, by taking the slopes of the lines of Figure S10 (see the Supporting Information), we find [Eq. (4)]:

$$\mathscr{D}_{Pr}^{obs} : \mathscr{D}_{Nd}^{obs} : \mathscr{D}_{Yb}^{obs} = +0.22 : -0.12 : 1 \quad (4)$$

This shows that whereas Nd and Yb binolam complexes match Bleaney's ratio reasonably well, $[Pr(binolam)_3]\cdot(OTf)_3$ (**3**) has a completely different magnetic susceptibility anisotropy. Such a behaviour is extreme, because of the sign inversion, and we can interpret it as due to the fact that the Pr nucleus in **3** has a higher coordination number than expected: residual water may be a good candidate, as in many other similar cases.[32,33] Remarkable variations in the $\mathscr{D}$ values due to different axial coordination in chelates, in which a macrocyclic ligand occupies only an equatorial region leaving the space above and below $Ln^{3+}$, have been reported previously.[34,35]

We must conclude that isostructurality holds for the organic part of the complexes, and not only does binolam have the same conformation, but also the three moieties are equally organised around $Ln^{3+}$ independent of the lanthanide.[36]

One final question to address is the location of the hydroxyl proton. We observed a broad downfield signal assigned to this species. Unfortunately, it may be affected by a considerable contact contribution (if it resides on oxygen, it is only two bonds away from the $Ln^{3+}$) and moreover possibly subject to exchange with residual water. These two facts make the separation of a reliable $\delta^{pc}$ or relaxation rate very difficult and this was not attempted.

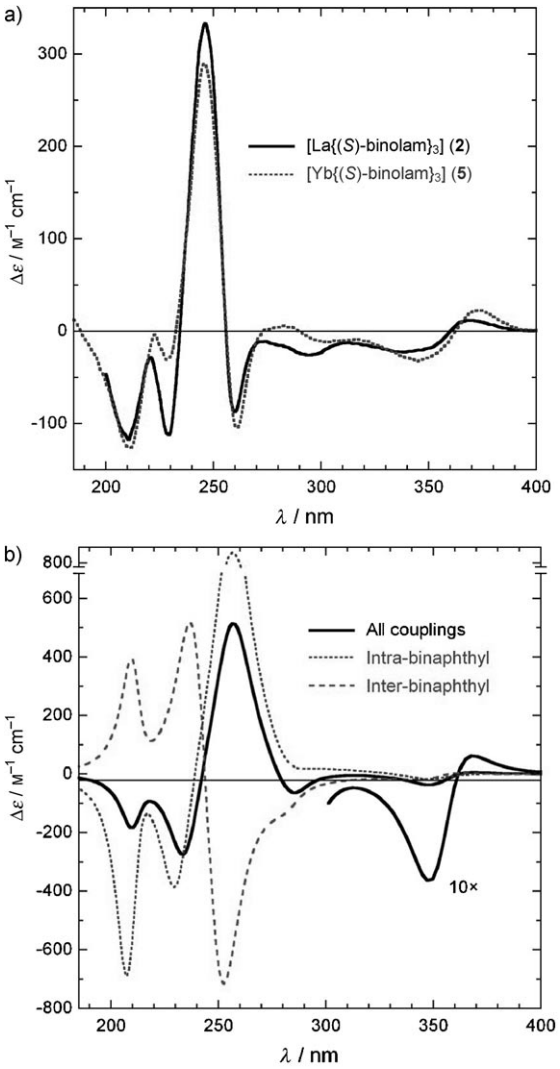


Figure 8. a) CD spectra of $[La\{(S)\text{-binolam}\}_3]\cdot(OTf)_3$ (**2**) and $[Yb\{(S)\text{-binolam}\}_3]\cdot(OTf)_3$ (**5**) in acetonitrile. b) CD spectra calculated for $[Yb\{(S)\text{-binolam}\}_3]\cdot(OTf)_3$ with the DeVoe method using the PERSEUS-derived best-fit structure.

**CD spectroscopy**: We can divide the analysis of the circular dichroism data into two main aspects: ligand and metal-centred CD.

We measured UV/Vis CD spectra for the enantiopure La and Yb binolam complexes **2** and **5**. The two spectra, shown in Figure 8, are quite similar and differ substantially from those of the free ligand (Figure 3). It has been demonstrated several times that the CD spectra of 1,1′-binaphthyl derivatives are very sensitive to the conformation of each binaphthyl unit as well as to the reciprocal arrangement of different binaphthyl units.[7,18,19,37–39] The first factor, and in particular the dihedral angle between the two naphthalene planes, affects the exciton coupling (named intra-binaphthylic) between directly attached naphthalene chromophores, whereas the second factor affects the coupling (named inter-binaphthylic) between more remote chromophores. Both types of coupling contribute to the observed spectrum, and for metal complexes containing multiple binol(ate) units the inter-binaphthylic term, although less strong than the intra-binaphthylic one, cannot be neglected.[7,40,41] The consistency between the CD spectra of La and Yb binolam complexes **2** and **5** represents a strong proof of substantial isostructurality along the series, as evidenced by NMR spectroscopy. On a more quantitative ground, the CD of these complexes may be calculated for a given structure and compared with the experimental one to afford detailed structural information. A reliable and inexpensive calculation approach consists of coupled-oscillator calculations run with the so-called DeVoe's method,[40,41] which has already been successfully applied to 1,1′-binaphthyl derivatives in many instances.[7,18,40–42] In the current case, the best-fit structure derived from PERSEUS for $[Yb\{(S)\text{-binolam}\}_3]\cdot(OTf)_3$ (**5**) was used as input structure. Spectral parameters for 2-naphthoate were considered as appropriate for depicting the aromatic

  

chromophore; they were taken from the literature[43] and from the absorption spectrum of **1** in acetonitrile and are summarised in the Experimental Section. The calculated spectrum (Figure 8b) is in very good agreement with the experimental spectra for both binolam complexes **2** and **5** in terms of overall shape. Thus, CD spectroscopy offers an independent proof of the validity of PERSEUS-based optimisation. By comparing the separate results for the intra- and inter-binaphthylic terms, it is clear that the former dominates the CD spectrum but the latter heavily contributes to the overall shape.

In the case of [Yb{(*S*)-binolam}$_3$]·(OTf)$_3$ (**5**), we also measured the metal-centred CD in the NIR region (see Figure 9). This spectral region is completely devoid of

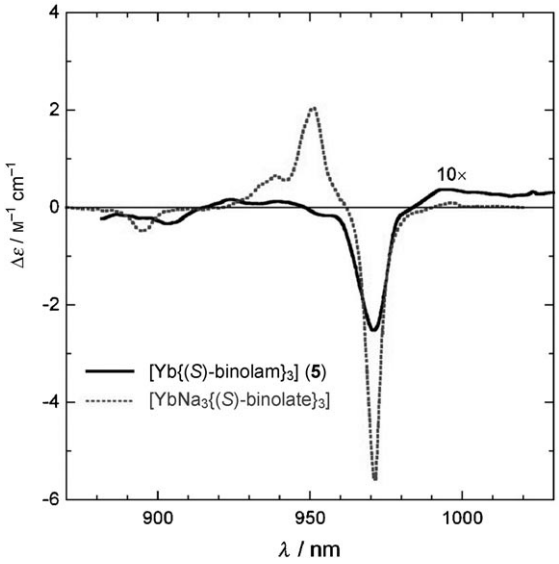


Figure 9. NIR CD spectrum of [(Δ,*S*,*S*,*S*)-Yb(binolam)$_3$] (**5**; ——) compared to that of (Λ,*S*,*S*,*S*)-YbNa$_3$ binolate (·····).

ligand-centred contributions of any kind (absorption and CD); thus, neither the free $Yb^{3+}$ (which is achiral) nor the free ligand can affect the observed spectrum. The NIR CD spectrum of [(Δ,*S*,*S*,*S*)-Yb(binolam)$_3$] is essentially reduced to one negative line at 970.8 nm, with $\Delta\varepsilon = -0.1$. Smaller features below and above this Cotton effect are very weak and confused with the baseline.

We can compare this NIR CD spectrum with the one obtained for (Λ,*S*,*S*,*S*)-YbNa$_3$ binolate, also shown in Figure 9. We can observe that in the case of [(Δ,*S*,*S*,*S*)-Yb(binolam)$_3$] (**5**), the NIR CD spectrum is much weaker and is of the same sign as (Λ,*S*,*S*,*S*)-YbNa$_3$ binolate.

**Dynamic features**: We can gain information on dynamic processes by using exchange spectroscopy (EXSY). The most prominent feature in EXSY is the exchange between the diastereotopic protons in the *N*-ethyl chains. In particular, the two methyl groups and the geminal protons at C10 do exchange. In the case of [La(binolam)$_3$]·(OTf)$_3$ (**2**), we quantified this process, by taking the relevant peak volumes and by analysing them with the routine EXSYcalc contained in MestReC,[44] thereby obtaining a rate constant of 0.25 $s^{-1}$. This value fits very well with variable-temperature data (not shown). This process must be associated with nitrogen inversion, which is rather surprising in view of its partial quaternisation and/or its involvement in a cyclic H-bond.

In samples showing traces of hydrolysis or when an excess of ligand was added, another network of cross peaks reveals that there is exchange between bound and free ligands (the latter being present as the triflate salt). The timescale of this process is around 1 $s^{-1}$, which is in close analogy with $M_3Ln$ binolates.[7]

The EXSY NMR spectrum of a 1:1 mixture of [La(binolam)$_3$]·(OTf)$_3$ (**2**) (racemic) and binolam **1** (racemic) in $CD_3CN$ shown in Figure S13 (see the Supporting Information) further confirmed these conclusions. In addition, this study showed that bound and free binolam units exchange easily, thus proving the kinetically labile nature of the complexes. Moreover, a spectrum obtained by diffusion-ordered spectroscopy (DOSY) of this 1:1 mixture showed the presence of two well-defined species having quite different diffusion parameters according to their dissimilar hydrodynamic radius (see the Supporting Information). Diffusion coefficient values *D* were obtained from the observed magnetic field intensity changes under gradient pulses, as reported by Pregosin and co-workers,[45] and these coefficients were then related to the hydrodynamic radius $r_H$ according to the Stokes–Einstein equation [Eq. (5)]:

$$r_H = kT/6\pi\eta D \qquad (5)$$

where $\eta$ is the solution viscosity, approximated by that of the solvent.

In addition, ligand exchange was easily observed when isotopically labelled ligand [$D_4$]binolam (readily available by $AlLiD_4$ reduction of the precursory amide) was added to a $CD_3CN$ solution of [La(binolam)$_3$]·(OTf)$_3$ (**2**) and its $^1$H NMR spectrum recorded. Immediately after the addition we observed the appearance in solution of unlabelled binolam, thus proving that the exchange is fast to the observer, though slow in the NMR timescale. The exchange rate was found to be highest for La, low for Yb, but null for Sc, in correlation with their decreasing coordination numbers.

We now know that free and bound ligand can exchange but, at the same time, that there is no trace of the existence of the heterochiral complex in the NMR spectrum. We may then wonder if we can observe the exchange between ligands of opposite configuration. If this is the case, on adding a large excess of (*R*)-binolam to 1 equiv of [(Δ,*S*,*S*,*S*)-Yb(binolam)$_3$] **5**, we should observe a variation in the NIR CD intensity and, ultimately, the inversion of the Cotton effect, as some of us reported in the case of $M_3Yb$ binolates.[6]

  

On running this experiment with six equivalents of the *R* ligand, initially we could not detect any significant variation of NIR CD intensity: only several minutes after the addition of the ligand of opposite configuration did we observe an evolution. Indeed, in this case the dynamics is very slow: the passage through NIR CD = 0 occurs at about time $t = 4$ h. The analysis of the curve of ellipticity $\theta_{971\,nm}$ as a function of time through Equation (6) yields $\tau = 5.5 \times 10^4$ s.

$$\theta(t) = \theta(\infty) + [\theta(0) - \theta(\infty)]e^{-t/\tau} \quad (6)$$

We observed that water plays a sort of catalytic role in this process: when the experiment was carried out under less accurate conditions, that is, without careful desiccation of solvent and glass- and quartz-ware, the evolution was faster. As this went out of the scope of our investigation we postponed any further work on the subject.

We may conclude this section by observing that we cannot completely exclude the presence of *some* heterochiral complex: a very small quantity may pass unnoticed in NMR spectroscopy, but it is the necessary intermediate stage for the observed dynamic NIR CD inversion.

**Studies on the catalytic processes promoted by [Ln(binolam)$_3$]·(OTf)$_3$ complexes**: The catalytic activity of enantiopure [(Δ,*S*,*S*,*S*)-Ln(binolam)$_3$] complexes has been demonstrated in previous work by some of us.[1,2] The published results clearly indicate that the La complex **2** in the presence of an equimolar amount of a strong base (either Proton Sponge (PS), tetramethyl guanidine (TMG), or 1,8-diazabicyclo[5,4,0]undec-7-ene (DBU) have been employed, the former being the most commonly used) is most efficient in promoting the nitroaldol (Henry) reaction, not only upon aldehydes but also, and most interestingly, upon trifluoromethyl ketones too (Scheme 3), though in this case a higher load of catalyst and base was required (25%).

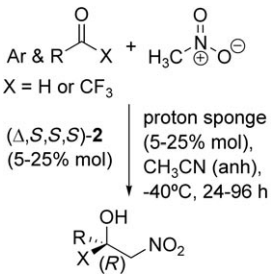


Scheme 3. Enantioselective nitroaldol reactions catalysed by [(Δ,*S*,*S*,*S*)-La(binolam)$_3$] complex **2**.

Compound **2** was chosen as the best lanthanide complex for catalysis after evaluation of the nitroaldol reaction of dihydrocinnamaldehyde with nitromethane in the absence of an external base. A strong decrease in chemical yield and enantioselectivity was noticed on passing from the lanthanum complex **2** (88%, 61% enantiomeric excess *ee*) to the scandium complex **6** (29%, 16% *ee*). The significant acceleration observed when adding an external base (1 equiv relative to lanthanide complex), such as binolam **1** (87% yield, 46% *ee*), suggested the need to explore even stronger bases. We attributed the partial erosion of the *ee* values observed to partial hydrolysis of **2** (which contains some residual water) in the presence of an external base, thereby giving rise to lanthanum hydroxide capable of promoting the background, racemic reaction. Actually, as mentioned above, careful addition of increasing amounts of water to complexes **2**–**6** dissolved in $CD_3CN$ leads to hydrolysis (fast for **2** but slower for the smaller lanthanides and scandium), thereby yielding binolammonium salt and the appropriate lanthanide hydroxide, which appears as a mucus-like flocculating species in the NMR tube. So, to promote catalysis in the presence of an external base one should be careful to avoid the presence of trace amounts of water in the reaction mixtures, a goal that is extremely difficult to reach. It needs to be emphasised in this respect that given the molecular mass of **2** (1805 g mol$^{-1}$), even 1% of water (18 g mol$^{-1}$) should have a deleterious effect on the complex if a base is present. Should water contamination reach the amount of 5%, then extensive hydrolysis will occur rapidly, thereby giving rise to $La(OH)_3$ and binolammonium triflate (3 equiv). With these precautions in mind, we learned that the optimum protocol for nitroaldol reactions called for the use of lanthanum complex **2** in the presence of an equimolar amount of PS dissolved in anhydrous acetonitrile at −40 °C, as already reported.[1,2]

Several points of interest in regard to the hypothetical mechanistic course of these reactions need to be discussed in advance. The first refers to the labile kinetic nature of the lanthanide complexes [Ln(binolam)$_3$]·(OTf)$_3$, which runs parallel to their capacity to expand the coordination number of the core lanthanide atom. In addition, it is worth recalling that a thermogravimetric analysis (25–200 °C) carried out with [La(binolam)$_3$]·(OTf)$_3$ (**2**) showed that a two-year-old sample kept in a closed vial was found to be contaminated with, for the most part, $H_2O$ (up to 4.6% in weight), as revealed by a careful IR study carried out with non-manipulated samples of **2** (self-supported pellets were employed for this purpose) and carefully dried up to 150 °C in a home-made quartz cell under high vacuum. Therefore, one has to accept that the actual samples employed for catalysing the above reactions may contain water and some residual acetonitrile as contaminants (in some cases up to 4.6%).

We used $^1$H, $^{13}$C and $^{19}$F NMR displacements as criteria for learning about the complexation of aldehydes (dihydrocinnamaldehyde) or trifluoromethyl ketones (1,1,1-trifluoro-2-butanone), as well as of nitromethane itself, with lanthanide complexes [Ln(binolam)$_3$]·(OTf)$_3$, for which purpose lanthanum (**2**), ytterbium (**5**) and praseodymium (**3**) complexes were employed. In this endeavour we found no clear-cut evidence, neither for complexation of aldehydes nor for complexation of trifluoromethyl ketones, nor even for the complexation of nitromethane. In addition, the ESI mass spectra of each of these mixtures did not show positive indi-

  

cations for complexation either. Accordingly, we next tried to establish the role of the added base.

NMR analysis of a solution of nitromethane in $CD_3CN$ in the presence of PS did not provide evidence for the formation of nitronate,[46,47] and thus we examined the role played by the external base upon the pre-catalysts $[La(binolam)_3]\cdot(OTf)_3$ (**2**) and $[Sc(binolam)_3]\cdot(OTf)_3$ (**6**) by NMR spectroscopy, as well as with ESI-MS, a technique that is being employed extensively for the study of complex catalytic mixtures.[48–54] According to the NMR analysis, addition of 1 equivalent of PS to a solution of the scandium complex **6** in $CD_3CN$ (commercial $CD_3CN$ contains some water) leads to removal of one of its protons (O-H-N), as revealed by the fact that the two diastereotopic methyl groups (of the $NEt_2$), which appeared as two triplets centred at $\delta=1.03$ and 0.61 ppm in **6**, collapsed into one triplet centred at $\delta=$ 0.82 ppm, together with the concomitant appearance of a signal at $\delta=3.2$ ppm which corresponds to the methyl groups of protonated PS ($PSH^+$). Addition of up to 3 equivalents of PS apparently did not induce further changes, the signals corresponding to both PS and $PSH^+$ being clearly observed (Figure S15, Supporting Information). Because the spectrum of PS in commercial $CD_3CN$ did not lead to the production of the ammonium salt of PS, even after the addition of water, we can conclude that the role played by PS upon **6** is the removal of one of its highly acidic hydrogen atoms, namely one O-H-N hydrogen, the resulting species retaining its overall $D_3$ symmetry presumably because of a series of fast internal proton transfers. ESI-MS analysis of a 1:3 mixture of **6** with PS in acetonitrile provided further evidence in favour of the removal of hydrogen atoms from the scandium complex **6** (Figure S16, Supporting Information). Actually, the ion of highest intensity (100%) in this mixture corresponds to the removal of three triflic acid moieties $[M-3TfOH+H]^+$ at *m/e* 1412.7697 mu (100%), in full accordance with the simulated spectrum that showed the corresponding peak at *m/e* 1412.7766 mu. Minor peaks at *m/e* 1561.7299 and *m/e* 1711.6930 (30 and 4%, respectively) correspond to the removal of two $[M-2TfOH+H]^+$ and one triflic acid moieties $[M-1TfOH+H]^+$, respectively. It is worth recalling that the ESI-MS spectrum of **6** shows peaks at *m/e* 1711.7095 (80%), 1561.7543 (35%) and 1255.4258 mu (100%). Thus, both NMR and ESI-MS data support the fact that addition of PS induces the removal of protons from complex **6**. In particular, according to the $^1H$ NMR spectrum there is a quantitative removal of one hydrogen atom, but we cannot exclude that removal of two or three hydrogen atoms might also take place, although in these cases the equilibrium should lie far to the left, that is, the resulting species are observed only by ESI-MS and not by NMR spectroscopy.

We have also examined the effect of adding PS to lanthanum complex **2** by means of NMR analysis (Figure S17) and ESI-MS (Figure S18, Supporting Information). Actually, the behaviour of **2** and **2**+PS (1–3 equiv) according to ESI-MS is parallel to that shown for **6** and **6**+PS. Thus, whereas **2** shows a highest intensity (100%) peak at *m/e* 1805.6195 mu, which corresponds to $[M-1TfOH+H]^+$, together with a low intensity (2%) peak at *m/e* 1655.6355 corresponding to $[M-2TfOH+H]^+$, the ESI-MS of **2**+PS (3 equiv) showed the highest peak (100%) at *m/e* 1505.7236 mu, which corresponds to $[M-3TfOH+H]^+$, together with small peaks at 1805.6191 (1%) and 1655.6586 (17%) due to $[M-1TfOH+H]^+$ and $[M-2TfOH+H]^+$, respectively. The ESI-MS of **2**+PS (1 or 2 equiv) led to intermediate spectra between both extremes. However, the NMR spectrum is somewhat more complicated and therefore leads to some ambiguity. Firstly, under the conditions of operation even trace amounts of water give rise to hydrolysis, thereby leading to free binolam and the ammonium ion of PS. Because **2** may contain up to 4.6% of water, its use without a specific drying protocol leads to extensive hydrolysis under these conditions. Worse than that, due to the high molecular weight of **2**, even carefully dried materials and solvents lead to hydrolysis to some extent. Secondly, equilibration appears to take place slowly after addition of PS and removal of hydrogen.

On the basis of the above experiments, the following mechanistic hypothesis (Scheme 4) can be proposed.

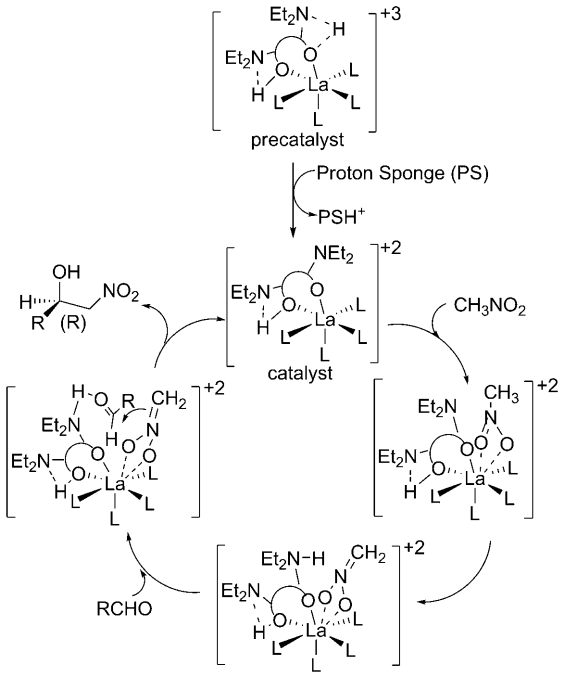


Scheme 4. Hypothetical mechanism for the Henry reaction of aldehydes (or trifluoromethyl ketones) catalysed by cationic lanthanum complex **2** in the presence of Proton Sponge (PS); one binolam unit has been schematically depicted, whereas the others are indicated through L (representing oxygen atoms).

1) Monodeprotonation of tricationic catalyst **2** possessing an arrayed acid–base network (LABABB) by means of an external amine (1 equiv of DBU or PS leads to a dicationic, monodeprotonated species **2**-H).
2) Nitromethane coordinates to the central lanthanum acting as Lewis acid (LA), the free diethylamino moiety

  

acting as Brønsted base (BB) in deprotonating it, thereby giving rise to a chiral lanthanum nitronate (we cannot rule out the possibility that this operation could be done by hydroxide ions).

3) We speculate that facial discrimination of the aldehyde or α-trifluoromethyl ketone may occur by coordination to the nearby ammonium moieties, thereby facilitating enantioselective condensation.
4) We also speculate that product release is the result of an internal proton transfer, thereby regenerating the active catalyst **2**-H again.

## Conclusion

Lanthanide salt complexes of general formula [Ln(binolam)$_3$]·(OTf)$_3$ (**2**–**6**) constitute a new class of compounds very different from those reported by Shibasaki. Enantiomerically pure (either Δ,*S*,*S*,*S* or Λ,*R*,*R*,*R*) complexes can be easily obtained as shelf-stable, chiral-at-metal compounds by simply mixing the appropriate dried lanthanide(III) triflate salt, or scandium(III) triflate salt, with enantiomerically pure binolam or binolamo in 1:3 ratio. No evidence has been found for the presence of other diastereomeric species when racemic binolam or binolamo were used for complexation. Kinetic lability appears to be responsible for this behaviour as well as for their hydrolysability. These compounds possess an extended array of acid and base sites (Lewis acid–Brønsted acid–Brønsted base or LABABB) that are presumably responsible for catalysis. Actually, the lanthanum complex **2** in the presence of a strong base such as PS appears to function as a pre-catalyst in promoting the enantioselective nitroaldol reaction of aldehydes and α-trifluoromethyl ketones, thereby giving rise to enantiomerically pure secondary or tertiary nitroalcohols. NMR and ESI-MS data suggest that the actual catalyst is a dicationic species **2**-H, in which at least one O-H-N hydrogen has been removed.

## Experimental Section

All measurements shown were carried out at least in duplicate on samples prepared each time from enantiopure and racemic binolam and Ln(TfO)$_3$, as described in references [1,2]. There is no appreciable difference in the NMR data of enantiopure or racemic material, nor in the data from different samples of the same species.

NMR spectra were recorded on a Varian Inova 600 spectrometer operating at 14.1 T and 25(±0.1) °C if not otherwise specified. For each sample, we estimated the longest $T_1$ and chose $3T_1$ as the relaxation delay. The assignments were performed through TOCSY (20 ms spin lock mixing) and HSQC ($J$ = 140 Hz) experiments. EXSY spectra were collected through the ROESY pulse sequence (mixing time 1 s, $B_1$ 3000 Hz) in the case of La complexes, through NOESY. The spectra where referred to the residual solvent resonances. To ascertain that we could exclude any shift due to (partial) coordination of acetonitrile to paramagnetic $Ln^{3+}$, mesitylene (1 μL) was added; the methyl and aromatic signal resonances ($^1$H and $^{13}$C) were constant. $^1$H DOSY experiments were performed with the DgcsteSL pulse sequence, with gradient pulses having 2 ms pulse width and 1.17–46.8 G cm$^{-1}$ strength.

UV/Vis CD spectra were recorded with a JASCO J-715 spectropolarimeter with a 0.01 cm cell for 0.1–0.7 mM acetonitrile solutions and under the following conditions: scan speed, 20 nm min$^{-1}$; response, 1 s; bandwidth, 1 nm.

NIR CD spectra were recorded with a JASCO J-200 D spectropolarimeter operating between 750 and 1350 nm, modified with a tandem Si/InGaAs detector with a dual photomultiplier amplifier, a 1 cm cell for 10 mM acetonitrile solutions, and under the following conditions: scan speed, 20 nm min$^{-1}$; bandwidth, 4 nm; time constant 4 s. Between 4 and 16 scans were accumulated to improve the signal-to-noise ratio.

**Computational details**: DFT calculations were run with Gaussian 03W,[55] by using the B3LYP hybrid functional which combines the three-parameter non-local hybrid exchange potential developed by Becke[56] with the LYP non-local correlation functional.[57] The 6-31+G(d+,p) basis set was obtained by adding an additional set of diffuse d polarisation functions to the standard 6-31+G(d,p) set, as suggested by Rablen et al. for treating hydrogen-bonded systems.[15] Geometry optimisations of lanthanum complexes were carried out using the 6-31G(d) basis set for all non-metallic atoms, and the Stuttgart/Dresden SDD effective-core-potential basis set for lanthanum. For this purpose, and to reduce the size of the catalysts for study, we simplified somewhat the binaphthalene ligand binolam by converting it into the biphenyl analogue "biphelam".[1,2]

DeVoe calculations on [La(binolam)$_3$]·(OTf)$_3$ (**5**) were run using a Fortran routine written by Hug et al.[58,59] Four π–π* transitions were considered for each naphthoate moiety in **5**, namely $^1L_b$ (352 nm), $^1L_a$ (284 nm), $^1B_b$ (241 nm), and $^1B_a$ (211 nm). Spectral parameters (transition frequency, dipolar strength and bandwidth) were extracted from the UV spectrum of binolam in acetonitrile, and are summarised in Table S3 in the Supporting Information. Dipoles were placed in the middle of each naphthalene ring and their polarisation directions (also shown in Table S3, Supporting Information) were taken from those reported in the literature for the 2-naphthoate anion.[43]

## Acknowledgements

Financial support by the Ministerio de Ciencia e Innovación of Spain (CTQ2007–62952/BQU) and from the Ministero dell'Istruzione Università e della Ricerca of Italy (PRIN 2007PBWN44) are gratefully acknowledged. The authors acknowledge the assistance of Dr. A. L. Llamas-Saiz (USC) and Dr. Angel Alvarez (UAB) in obtaining the X-ray structures reported. CESCA and CESGA are thanked for their allocation of computer time. Thanks are also due to the Govern de les Illes Balears for a fellowship to J.M. L.D.B gratefully acknowledges a sabbatical granted by the Ministry of Science and Innovation of Spain.

[1] F. Tur, J. M. Saá, *Org. Lett.* **2007**, *9*, 5079–5082.
[2] J. M. Saá, F. Tur, J. Gonzalez, M. Vega, *Tetrahedron: Asymmetry* **2006**, *17*, 99–106.
[3] H. Sasai, T. Suzuki, S. Arai, T. Arai, M. Shibasaki, *J. Am. Chem. Soc.* **1992**, *114*, 4418–4420.
[4] M. Shibasaki, H. Sasai, T. Arai, *Angew. Chem.* **1997**, *109*, 1290–1311; *Angew. Chem. Int. Ed. Engl.* **1997**, *36*, 1236–1256.
[5] H. C. Aspinall, J. F. Bickley, J. L. M. Dwyer, N. Greeves, R. V. Kelly, A. Steiner, *Organometallics* **2000**, *19*, 5416–5423.
[6] L. Di Bari, M. Lelli, P. Salvadori, *Chem. Eur. J.* **2004**, *10*, 4594–4598.
[7] L. Di Bari, M. Lelli, G. Pintacuda, G. Pescitelli, F. Marchetti, P. Salvadori, *J. Am. Chem. Soc.* **2003**, *125*, 5549–5558.
[8] A. J. Wooten, P. J. Carroll, P. J. Walsh, *J. Am. Chem. Soc.* **2008**, *130*, 7407–7419.
[9] C. Nájera, J. Sansano, J. M. Saá, *Eur. J. Org. Chem.* **2009**, 2385–2400.
[10] Only a very small trace of the 1:1 complex can be detected when working with low ligand-to-metal ratios.

  

[11] J. M. Saá, F. Tur, J. González, *Chirality* **2009**, *21*, 836–842.
[12] F. Eckert, I. Leito, I. Kaljurand, A. Kütt, A. Klamt, M. Diedenhofen, *J. Comput. Chem.* **2009**, *30*, 799–810.
[13] I. Kaljurand, A. Kutt, L. Soovali, T. Rodima, V. Maemets, I. Leito, I. A. Koppel, *J. Org. Chem.* **2005**, *70*, 1019–1028.
[14] CCDC-768175; see ref. [28].
[15] P. R. Rablen, J. W. Lockman, W. L. Jorgensen, *J. Phys. Chem. A* **1998**, *102*, 3782–3797.
[16] N. Harada K. Nakanishi, *Circular Dichroic Spectroscopy—Exciton Coupling in Organic Stereochemistry*, University Science Books, Mill Valley, CA, **1983**.
[17] L. Di Bari, G. Pescitelli, P. Salvadori, *J. Am. Chem. Soc.* **1999**, *121*, 7998–8004.
[18] S. F. Mason, R. H. Seal, D. R. Roberts, *Tetrahedron* **1974**, *30*, 1671–1682.
[19] M. Rubio, M. Merchán, E. Ortí, B. O. Roos, *Chem. Phys.* **1994**, *179*, 395–409.
[20] K. Nishimoto, *J. Phys. Chem.* **1963**, *67*, 1443–1446.
[21] Y. Tanizaki, S.-i. Kubodera, *J. Mol. Spectrosc.* **1967**, *24*, 1–18.
[22] D. Andrae, U. Häußermann, M. Dolg, H. Stoll, H. Preuß, *Theor. Chim. Acta* **1990**, *77*, 123–141.
[23] It is well known that the presence of an external amine and traces of water cause the hydrolysis of lanthanide(III) salts. The reaction that occurs is: $LnX_3 + H_2O + NR_3 \rightarrow Ln(OH)_3 + R_3NHX$. See, for example: W. J. Evans, M. S. Sollberger, T. P. Hanusa, *J. Am. Chem. Soc.* **1988**, *110*, 1841–1850.
[24] L. Di Bari, P. Salvadori, *Coord. Chem. Rev.* **2005**, *249*, 2854–2879.
[25] I. Bertini, C. Luchinat, *Coord. Chem. Rev.* **1996**, *150*.
[26] We could not detect the resonances of quaternary carbon atoms, such as C2 and C3, which may also experience a considerable contact shift.
[27] Isostructurality between the various heterobimetallic complexes involving Li, Na or K was demonstrated in reference [7], in which it was shown that the pseudo-contact shifts for these three complexes are proportional. Thus, here it does not make any difference to refer specifically to one or the other.
[28] The structure obtained from single-crystal X-ray diffraction analysis displays positional disorder for the scandium cation. The main site is located at the centre of the complex and the minor ones are located in the pseudo-equivalent octahedral coordinated positions at each site of the main one. The refined occupation parameters are 0.912(2), 0.056(2) and 0.0037(2), respectively. CCDC-768175 and CCDC-768176 contain the supplementary crystallographic data for this paper. These data can be obtained free of charge from The Cambridge Crystallographic Data Centre via www.ccdc.cam.ac.uk/data_request/cif.
[29] S. Ripoli, S. Scarano, L. Di Bari, P. Salvadori, *Bioorg. Med. Chem.* **2005**, *13*, 5181–5188.
[30] B. Bleaney, *J. Magn. Reson.* **1972**, *8*, 91–100.
[31] V. S. Mironov, Y. G. Galyametdinov, A. Ceulemans, C. Gorller-Walrand, K. Binnemans, *J. Chem. Phys.* **2002**, *116*, 4673–4685.
[32] S. Aime, M. Botta, M. Fasano, M. P. M. Marques, C. F. G. C. Geraldes, D. Pubanz, A. E. Merbach, *Inorg. Chem.* **1997**, *36*, 2059–2068.
[33] F. A. Dunand, R. S. Dickins, D. Parker, A. E. Merbach, *Chem. Eur. J.* **2001**, *7*, 5160–5167.
[34] J. Lisowski, S. Ripoli, L. Di Bari, *Inorg. Chem.* **2004**, *43*, 1388–1394.
[35] L. Di Bari, G. Pintacuda, P. Salvadori, R. S. Dickins, D. Parker, *J. Am. Chem. Soc.* **2000**, *122*, 9257–9264.
[36] Naturally this is only a first approximation, because the Ln–O distances must be different according to lanthanide contraction: E. A. Quadrelli, *Inorg. Chem.* **2002**, *41*, 167–169.
[37] L. Di Bari, G. Pescitelli, G. Reginato, P. Salvadori, *Chirality* **2001**, *13*, 548–555.
[38] G. Pescitelli, L. Di Bari, P. Salvadori, *Organometallics* **2004**, *23*, 4223–4229.
[39] G. Pescitelli, L. Di Bari, P. Salvadori, *J. Organomet. Chem.* **2006**, *691*, 2311–2318.
[40] H. DeVoe, *J. Chem. Phys.* **1964**, *41*, 393–400.
[41] H. DeVoe, *J. Chem. Phys.* **1965**, *43*, 3199–3208.
[42] C. Koukoulitsa, A. Karioti, M. C. Bergonzi, G. Pescitelli, L. Di Bari, H. Skaltsa, *J. Agric. Food Chem.* **2006**, *54*, 5388–5392.
[43] T. Hoshi, J. Yoshino K. Hayashi, *Z. Phys. Chem. (Muenchen Ger.)* **1973**, *83*, 31–40.
[44] J. C. Cobas, M. Martin-Pastor, EXSyCalc, Version 1.0, MestReC, **2004**.
[45] P. S. Pregosin, P. G. A. Kumar, I. Fernandez, *Chem. Rev.* **2005**, *105*, 2977–2998.
[46] P. H. Boyle, M. A. Convery, A. P. Davis, G. D. Hosken, B. A. Murray, *J. Chem. Soc. Chem. Commun.* **1992**, 239–242.
[47] E. van Aken, H. Wynberg, F. van Bolhuis, *J. Chem. Soc. Chem. Commun.* **1992**, *629*–630.
[48] W. Schrader, P. P. Handayani, J. Zhou, B. List, *Angew. Chem.* **2009**, *121*, 1491–1494; *Angew. Chem. Int. Ed.* **2009**, *48*, 1463–1466.
[49] C. Markert, M. Neuburger, K. Kulicke, M. Meuwly, A. Pfaltz, *Angew. Chem.* **2007**, *119*, 5996–5999; *Angew. Chem. Int. Ed.* **2007**, *46*, 5892–5895.
[50] A. M. Cesar, F. Francesco, O. M. Jürgen, *Angew. Chem.* **2007**, *119*, 7040–7042; *Angew. Chem. Int. Ed.* **2007**, *46*, 6915–6917.
[51] L. S. Santos, C. H. Pavam, W. Almeida, P. F. Coelho, M. N. Eberlin, *Angew. Chem.* **2004**, *116*, 4430–4433; *Angew. Chem. Int. Ed.* **2004**, *43*, 4330–4333.
[52] C. Markert, A. Pfaltz, *Angew. Chem.* **2004**, *116*, 2552–2554; *Angew. Chem. Int. Ed.* **2004**, *43*, 2498–2500.
[53] A. A. Sabino, A. H. L. Machado, C. R. D. Correia, M. N. Eberlin, *Angew. Chem.* **2004**, *116*, 2568–2572; *Angew. Chem. Int. Ed.* **2004**, *43*, 2514–2518.
[54] P. Chen, *Angew. Chem.* **2003**, *115*, 2938–2954; *Angew. Chem. Int. Ed.* **2003**, *42*, 2832–2847.
[55] Gaussian 03, Revision D.01, M. J. Frisch, G. W. Trucks, H. B. Schlegel, G. E. Scuseria, M. A. Robb, J. R. Cheeseman, J. A., Montgomery, Jr., T. Vreven, K. N. Kudin, J. C. Burant, J. M. Millam, S. S. Iyengar, J. Tomasi, V. Barone, B. Mennucci, M. Cossi, G. Scalmani, N. Rega, G. A. Petersson, H. Nakatsuji, M. Hada, M. Ehara, K. Toyota, R. Fukuda, J. Hasegawa, M. Ishida, T. Nakajima, Y. Honda, O. Kitao, H. Nakai, M. Klene, X. Li, J. E. Knox, H. P. Hratchian, J. B. Cross, C. Adamo, J. Jaramillo, R. Gomperts, R. E. Stratmann, O. Yazyev, A. J. Austin, R. Cammi, C. Pomelli, J. W. Ochterski, P. Y. Ayala, K. Morokuma, G. A. Voth, P. Salvador, J. J. Dannenberg, V. G. Zakrzewski, S. Dapprich, A. D. Daniels, M. C. Strain, O. Farkas, D. K. Malick, A. D. Rabuck, K. Raghavachari, J. B. Foresman, J. V. Ortiz, Q. Cui, A. G. Baboul, S. Clifford, J. Cioslowski, B. B. Stefanov, G. Liu, A. Liashenko, P. Piskorz, I. Komaromi, R. L. Martin, D. J. Fox, T. Keith, M. A. Al-Laham, C. Y. Peng, A. Nanayakkara, M. Challacombe, P. M. W. Gill, B. Johnson, W. Chen, M. W. Wong, C. Gonzalez, J. A. Pople, Gaussian, Inc. Wallingford CT, **2004**.
[56] A. D. Becke, *J. Chem. Phys.* **1993**, *98*, 5648–5652.
[57] C. Lee, W. Yang R. G. Parr, *Physiol. Res.* **1988**, *37*, 785.
[58] W. Hug, F. Ciardelli, I. Tinoco, *J. Am. Chem. Soc.* **1974**, *96*, 3407–3410.
[59] C. L. Cech, W. Hug, I. J. Tinoco, *Biopolymers* **1976**, *15*, 131–152.

Received: June 14, 2010
Published online: October 18, 2010

  